International Journal of Control and Automation
Vol.9, No.2 (2016), pp.179-190
http://dx.doi.org/10.14257/ijca.2016.9.2.17

Tightly Coupled Integration of a Low Cost MEMS-INS/GPS System using Adaptive Kalman Filtering

Khan Badshah[1] and Qin Yongyuan[2]

School of Automation, Northwestern Polytechnical University, Xi'an Shaanxi 710072, P.R. China
[1]khan_phys@yahoo.com, [2]qinyongyuan@nwpu.edu.cn

Abstract

The integration of Inertial Navigation System (INS) and Global Positioning System (GPS) can produce accurate results if four or more GPS satellites are tracked. However, in GPS attenuated signal environment the errors of a low accuracy MEMS/GPS system rapidly grow to the unacceptable level. A tightly coupled integration scheme is utilized to improve the performance and reliability of the low accuracy integrated system in the areas such as tunnels, tall buildings, urban canyon, and forest canopy. This model is capable to detect the GPS fault and to track the errors of the integrated system even when less than four satellites are being tracked. Practically in INS/GPS integration, the system noises are not known correctly. Therefore, an Adaptive Kalman filter is proposed to merge the data of the two systems accurately. The algorithms are tested using the real data of MEMS-IMU (STIM300) and a single frequency NovAtel GPS receiver for land navigations. The integration results indicate a significant improvement in the accuracy of attitude, velocity and position parameters. Moreover, gyro drift which is the main source of errors in INS parameters is significantly reduced.

Keywords*: INS, IMU, MEMS, GPS, Pseudo range, Kalman Filter, Integration*

1. Introduction

The recent advancement in MEMS technology has made possible the development of a low cost, light weight and small size inertial sensors [1]. MEMS technology has enabled to build a complete Inertial Measurement Unit (IMU) on a small chip composed of multiple integrated MEMS accelerometers and gyroscopes [2]. However, due to incomplete maturity of this technology, the performance and reliability of these sensors is limited [3]. These IMUs do not meet the accuracy requirement of many navigation applications [4]. Therefore, MEMS are augmented with other navigation aids to enhance their performance and reliability by reducing their fast errors growth to the acceptable accuracy level. Nowadays, inexpensive and single-chip GPS receivers are available in the market, which are being increasingly utilized in many consumer products such as car navigation, cellular phones, personal digital assistants, and security devices [5]. The combination of GPS and MEMS-INS offers a low cost, light weight and sufficiently accurate and reliable solution for many navigation applications [6].

GPS can restrict INS error growth over time, while the INS can enhance the reliability and integrity of the system [7]. Therefore, the navigation solution derived from INS/GPS system is better than either stand-alone system [8]. Loosely coupled model has limited application due to the requirement of four visible satellites at least. Therefore, this scheme has best implementation results with higher quality INS systems. Contrary to this, MEMS based IMUs are suited only for applications where GPS outages are infrequent and short in duration [8]. In tightly coupled scheme, the raw pseudo-range and pseudo-range rate tracking loop

ISSN: 2005-4297 IJCA

output and those from INS prediction are combined to form the input of the centralized integration filter. The filter directly accepts their differences to obtain the INS error estimates [9]. It can continue to generate integrated navigation solution even when fewer than four satellites are being tracked. Therefore, this integration strategy is a preferred approach to utilize for land navigation vehicles where chance of satellite signal blockage is higher due to tall buildings, trees and tunnels etc.

INS and GPS sensors data are typically blended using the Conventional Kalman filter (CKF).The CKF works well and produce optimal results if the process and measurement noises are known [10]. In practical, these matrices are unknown or approximated by applying the best available knowledge which may results in unreliable performance or causes the CKF to diverge. The classical approach that chooses the values for these two matrices is through empirical analysis of the process and measurement errors or to set them manually in an ad hoc fashion. The modification of this stochastic information used within CKF is known as Adaptive Kalman filtering (AKF). Sage-Husa AKF is proposed to implement in this integration which makes various modifications to the CKF algorithm that allow the filter to modify the stochastic information on-line for best optimal estimation and convergence of the filter [11,12].

2. INS Errors Dynamics

Fundamental to the mechanization of inertial navigation and its error analysis is the precise definition of a number of Cartesian co-ordinate reference frames. Each frame is an orthogonal, right-handed co-ordinate frame. Inertial frame (*i*-frame) has its origin at the center of the earth and is non-rotating with respect to the fixed stars, as shown in Fig-1. Earth frame *(e*-frame), also called earth centered earth fixed frame (ECEF), is a coordinate frame which has its origin at the earth's center of mass and has axes which are fixed in the earth. The axes of inertial and earth frames are arranged such that they are coincident at navigation starting time, $t = 0$ as shown in Fig-1. Navigation frame (*n*-frame) is a local level geographic frame at the system location. East-North-Up (ENU) frame is used as a local level navigation frame in this work. The body frame (*b*-frame) is the frame in which the accelerations and angular rates generated by INS are resolved. Its x-axis points toward right, y-axis along the vehicle longitudinal axis and z-axis is upward completing the right-handed system [13- 15].

The INS linear errors dynamics is expressed by the differential equations describing the attitude, velocity and position errors states referenced to a local level navigation frame (ENU). These differential equations are expressed as [16].

$$\dot{\phi} = -\omega_{in}^{n} \times \phi + \delta\omega_{in}^{n} - C_{b}^{n}\varepsilon^{b} \qquad (1)$$

$$\delta\dot{v}^{n} = -\phi \times C_{b}^{n} f_{sf}^{b} - (2\omega_{ie}^{n} + \omega_{en}^{n}) \times \delta v^{n} - (2\delta\omega_{ie}^{n} + \delta\omega_{en}^{n}) \times v^{n} + C_{b}^{n}\nabla^{b} \qquad (2)$$

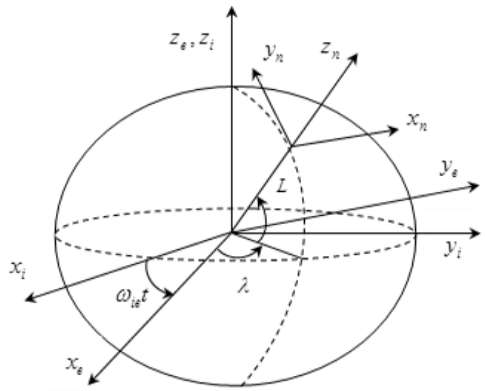

Figure 1. Coordinate frames

$$\left.\begin{aligned} \delta\dot{L} &= \frac{1}{R_M + h}\delta v_N^n - \frac{v_N^n}{(R_M + h)^2}\delta h \\ \delta\dot{\lambda} &= \frac{\sec L}{R_N + h}\delta v_E^n - \frac{v_E^n \sec L \tan L}{R_N + h}\delta L - \frac{v_E^n \sec L}{(R_N + h)^2}\delta h \\ \delta\dot{h} &= \delta v_U^n \end{aligned}\right\} \quad (3)$$

Where $\phi = \begin{bmatrix}\phi_E & \phi_N & \phi_U\end{bmatrix}^T$, $\delta v^n = \begin{bmatrix}\delta v_E^n & \delta v_N^n & \delta v_U^n\end{bmatrix}^T$ and $\delta p = \begin{bmatrix}\delta L & \delta\lambda & \delta h\end{bmatrix}^T$ are attitude, velocity and position error vectors. The symbol "$\times$" represents the skew-symmetric matrix of the vector. Whereas ε^b, ∇^b are gyro drift and accelerometer bias errors, respectively. Accelerometer and gyroscopes fixed biases can be represented by trivial differential equations

$$\left.\begin{aligned} \dot{\varepsilon}^b &= \begin{bmatrix}\dot{\varepsilon}_x^b & \dot{\varepsilon}_y^b & \dot{\varepsilon}_z^b\end{bmatrix}^T = 0 \\ \dot{\nabla}^b &= \begin{bmatrix}\dot{\nabla}_x^b & \dot{\nabla}_y^b & \dot{\nabla}_z^b\end{bmatrix}^T = 0 \end{aligned}\right\} \quad (4)$$

3. INS/GPS Tightly Coupled Model

In tightly coupled architecture the pseudo-range and pseudo range rate of the GPS receiver is fused with the lower precision INS data to correct the navigation parameters. The orientation of the satellite and a GPS receiver installed on an aircraft is shown in Fig-2. Position of the ith satellite (p_{si}) and the GPS receiver (p_r) in ECEF coordinate frame are defined as

$$p_{si} = \begin{bmatrix}x_{si} & y_{si} & z_{si}\end{bmatrix}^T$$

$$p_r = \begin{bmatrix}x_r & y_r & z_r\end{bmatrix}^T$$

The position vector and its change rate from the receiver to the satellite can be expressed as

$$r_i = p_{si} - p_r = \begin{bmatrix}x_{si} - x_r & y_{si} - y_r & z_{si} - z_r\end{bmatrix}^T$$

$$\dot{r}_i = \dot{p}_{si} - \dot{p}_r = \begin{bmatrix}\dot{x}_{si} - \dot{x}_r & \dot{y}_{si} - \dot{y}_r & \dot{z}_{si} - \dot{z}_r\end{bmatrix}^T$$

The corresponding pseudo range and the pseudo range rate from aircraft to the GPS receiver are written as

$$\left.\begin{array}{c} d_i = \|r_i\| \\ \dot{d}_i = d_i^{-1}(r_i^T \dot{r}_i) \end{array}\right\} \quad (5)$$

Where d_i is the true pseudo range. The pseudo range measurement ($\rho_{gps,i}$) can be modeled by the following expression [17, 18].

$$\rho_{gps,i} = d_i + c\delta t_r - c\delta t_s + cI_i + cT_i + \varepsilon_\rho \quad (6)$$

Where c is the velocity of light, δt_r and δt_s are receiver and satellite clocks errors. I_i and T_i are ionospheric and tropospheric errors whereas ε_ρ is the receiver white noise. After compensating the common mode errors and the satellite clock error the pseudo range model is written as

$$\rho_{gps,i} = d_i + c\delta t_r + \varepsilon_\rho \quad (7)$$

The pseudo range rate is obtained from the Doppler measurements as

$$\dot{\rho}_{gps,i} = d_i^{-1}\left\|r_i^T \dot{r}_i\right\| + c\delta \dot{t}_d + \varepsilon_{\dot{\rho}} \quad (8)$$

The receiver clock error and its drift are included in the error states and can be modeled by random walk

$$\left.\begin{array}{c} \delta \dot{b}_r = \delta d_r + w_b(t) \\ \delta \dot{d}_r = w_d(t) \end{array}\right\} \quad (9)$$

Here $\delta b_r = c\delta t_r$ and $\delta d_r = c\delta \dot{t}_r$ are clock bias and clock drift errors and w_b , w_d are their corresponding random noises. Equation-9 is further simplified as

$$\begin{bmatrix} \delta \dot{b}_r \\ \delta \dot{d}_r \end{bmatrix} = \begin{bmatrix} 0 & 1 \\ 0 & 0 \end{bmatrix} \begin{bmatrix} \delta b_r \\ \delta d_r \end{bmatrix} + \begin{bmatrix} w_b \\ w_d \end{bmatrix}$$

$$\dot{x}_{gps} = F_{gps} x_{gps} + W_{gps} \quad (10)$$

Receiver position computed from INS is always in geodetic coordinate (L, λ, h) which must be transformed into the ECEF farme to correlate with GPS measurements

$$p_{ins,r} = \begin{bmatrix} x_{ins,r} \\ y_{ins,r} \\ z_{ins,r} \end{bmatrix} = \begin{bmatrix} R_{Nh} \cos L \cos \lambda \\ R_{Nh} \cos L \sin \lambda \\ [R_N(1-e^2) + h] \sin L \end{bmatrix} \quad (11)$$

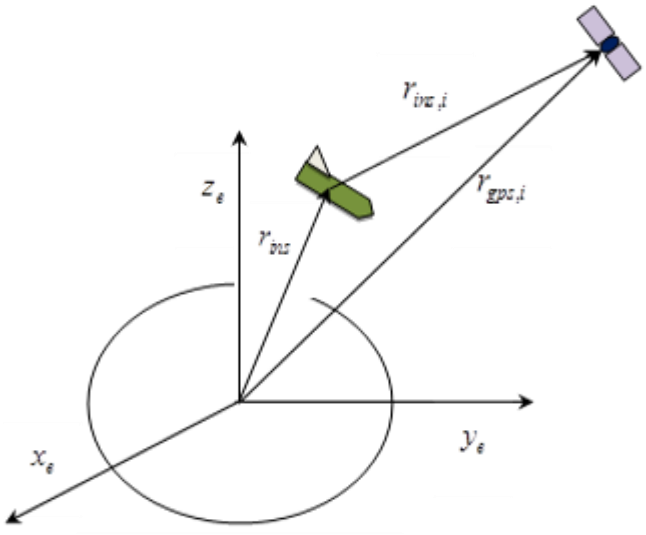

Figure 2. Satelite Geometry

Similarly the velocity can be transformed from n-frame into the ECEF frame

$$v^e_{ins,r} = C^e_n v^n_{ins.r}$$

Where

$$C^e_n = \begin{bmatrix} -\sin\lambda & -\sin L\cos\lambda & \cos L\cos\lambda \\ \cos\lambda & -\sin L\sin\lambda & \cos L\sin\lambda \\ 0 & \cos L & \sin L \end{bmatrix}$$

The relationship between position error in e-frame and n-frame is given by

$$\begin{bmatrix} \delta x_{ins,r} \\ \delta y_{ins,r} \\ \delta x_{ins,r} \end{bmatrix} = C_{err} \begin{bmatrix} \delta L \\ \delta\lambda \\ \delta h \end{bmatrix} \qquad (12)$$

Where C_{err} is calculated as

$$C_{err} = \begin{bmatrix} -R_{Nh}\sin L\cos\lambda & -R_{Nh}\cos L\sin\lambda & \cos L\cos\lambda \\ -R_{Nh}\sin L\sin\lambda & -R_{Nh}\sin L\cos\lambda & \cos L\sin\lambda \\ -R_{Nh}(1-e^2)\cos L & 0 & \sin L \end{bmatrix}$$

Similarly the velocity error in two frames are related as

$$\delta v^e_{ins,r} = C^e_n \delta v^n_{ins,r} \qquad (13)$$

Using the INS position $p_{ins,r}$ and velocity $v^e_{ins,r}$, the vector from GPS receiver to the ith satellite and its change rate can be calculated as

$$r_{ins,i} = p_{si} - p_{ins,r}$$

$$\dot{r}_{ins,i} = \dot{p}_{si} - \dot{p}_{ins,r}$$

Further, the pseudo range and pseudo range rate from INS data are estimated as follows [17]

$$\left.\begin{aligned} \rho_{ins,i} &= \left\| r_{ins,i} \right\| \\ \dot{\rho}_{ins,i} &= \rho_{ins,i}^{-1} (r_{ins,i}^T \dot{r}_{ins,i}) \end{aligned}\right\} \quad (14)$$

Expanding $\rho_{gps,i}$ and $\dot{\rho}_{gps,i}$ about INS computed position ($X_p = p_{ins,r}$) and velocity ($X_v = v_{ins,r}^e$) using Taylor series, we get

$$\left.\begin{aligned} \rho_{gps,i} &= \rho_{ins,i} + M_i \delta X_p + \delta b_r \\ \dot{\rho}_{gps,i} &= \dot{\rho}_{ins,i} + G_i \delta X_p + H_i \delta X_v + \delta d_r \end{aligned}\right\} \quad (15)$$

Where the matrices in Equation 16 are given as

$$M_i = \left.\frac{\partial \rho_{gps,i}}{\partial X_p}\right|_{p_{ins,r}} = \rho_{ins,i}^{-1} r_{ins,i}^T$$

$$H_i = \left.\frac{\partial \dot{\rho}_{gps,i}}{\partial X_v}\right|_{p_{ins,r}, v_{ins,r}^e} = -\rho_{ins,i}^{-1} r_{ins,i}^T$$

$$G_i = \left.\frac{\partial \dot{\rho}_{gps,i}}{\partial X_v}\right|_{p_{ins,r}, v_{ins,r}^e} = \frac{r_{ins,i}^T \dot{r}_{ins,i}}{\rho_{ins,i}^3} . r_{ins,v}^T - \frac{\dot{r}_{ins,i}^T}{\rho_{ins,i}}$$

Taking the difference of $\rho_{ins,i}$ and $\rho_{gps,i}$, together with the difference of $\dot{\rho}_{ins,i}$ and $\dot{\rho}_{gps,i}$ to get the measurements model of the tightly coupled integrated scheme

$$z_k = \begin{bmatrix} \rho_{ins,i} - \rho_{gps,i} & \dot{\rho}_{ins,i} - \dot{\rho}_{gps,i} \end{bmatrix}^T + v_k \quad (16)$$

Where v_k is the measurement noise which is mainly composed of GPS noise in pseudo range and pseudo range rate, with some small error components due to linearization process. All these errors are assumed to be uncorrelated white noises with zero mean and covariance matrix R_k . Substituting Eqs-17 and 18 in Eq-19 to get the measurement model

$$z_k = \begin{bmatrix} -M_i \delta X_p - \delta b_r \\ -G_i \delta X_p - H_i \delta X_r - \delta d_r \end{bmatrix} + v_k \quad (17)$$

$$z_k = \begin{bmatrix} -M_i C_{err} \delta p_{ins,r} - \delta b_r \\ -G_i C_{err} \delta p_{ins,r} - H_i C_n^e v_{ins}^r - \delta d_r \end{bmatrix} + v_k$$

$$z_k = \begin{bmatrix} 0_{1\times3} & 0_{1\times3} & -M_i C_{err} & 0_{1\times3} & 0_{1\times3} & -1 & 0 \\ 0_{1\times3} & -H_i C_n^e & -G_i C_{err} & 0_{1\times3} & 0_{1\times3} & 0 & -1 \end{bmatrix} x_k + v_k$$

$$x_k = \begin{bmatrix} \phi^T & (\delta v_{ins}^r)^T & (\delta p_{ins,r})^T & \varepsilon^b & \nabla^b & \delta b_r & \delta d_r \end{bmatrix}^T$$

$$z_k = H_k x_k + v_k \quad (18)$$

If there are *m* number of effective satellites available at time t_k then the measurements vector and the corresponding measurement model for tightly coupled integrated scheme is developed as

$$z_k = \begin{bmatrix} \delta\rho_1 & \delta\rho_2 & \cdots & \delta\rho_m & \delta\dot{\rho}_1 & \delta\dot{\rho}_2 & \cdots & \delta\dot{\rho}_m \end{bmatrix}^T + v_k \qquad (19)$$

Here $i = 1, 2, ...m$ and the sensitive matrix for *m* number of satellites is thus obtained as

$$H_k = \begin{bmatrix} 0_{1\times3} & 0_{1\times3} & -M_1 C_{err} & 0_{1\times3} & 0_{1\times3} & -1 & 0 \\ 0_{1\times3} & 0_{1\times3} & -M_2 C_{err} & 0_{1\times3} & 0_{1\times3} & -1 & 0 \\ \vdots & \vdots & \vdots & \vdots & \vdots & \vdots & \vdots \\ 0_{1\times3} & 0_{1\times3} & -M_m C_{err} & 0_{1\times3} & 0_{1\times3} & -1 & 0 \\ 0_{1\times3} & -H_1 C_n^e & -G_1 C_{err} & 0_{1\times3} & 0_{1\times3} & 0 & -1 \\ 0_{1\times3} & -H_2 C_n^e & -G_2 C_{err} & 0_{1\times3} & 0_{1\times3} & 0 & -1 \\ \vdots & \vdots & \vdots & \vdots & \vdots & \vdots & \vdots \\ 0_{1\times3} & -H_m C_n^e & -G_m C_{err} & 0_{1\times3} & 0_{1\times3} & 0 & -1 \end{bmatrix}$$

4. Sage-Husa AKF for INS/GPS

In the process of CKF the process and measurement noise matrices remain constant whereas in Sage-Husa AKF the states are estimated by innovations and are updated in real time. INS attitude, velocity, position and sensor errors are selected as the errors states of the system. The system error model can be expressed in the form of linear stochastic equations

$$\dot{x}(t) = Fx(t) + W(t)$$

$$x_k = \Phi_{k-1} x_{k-1} + \Gamma_{k-1} W_{k-1} \qquad (20)$$

$$z_k = H_k x_k + V_k \qquad (21)$$

The noises are assumed to be Gaussian with the following mean and covariance matrices

$$E(W_k) = q, Cov[W_k, W_j] = E[W_k W_j] = Q\delta_{k,j}$$

$$E(V_k) = r, Cov[V_k, V_j] = E[V_k V_j] = R\delta_{k,j}$$

$$Cov[W_k, W_j] = E[W_k W_j] = 0$$

The CKF estimates the states of the system as

$$\hat{x}_k^- = \Phi_k \hat{x}_{k-1} + \Gamma_{k-1} q_{k-1} \qquad (22)$$

$$P_k^- = \Phi_k P_{k-1} \Phi_k{}^T + \Gamma_{k-1} Q_{k-1} \Gamma_{k-1}^T \qquad (23)$$

$$\hat{x}_k = \hat{x}_k^- + K_k (z_k - H_k \Phi_k \hat{x}_k^- - r_k) \qquad (24)$$

$$K_k = P_k^- H_k{}^T (H P_k^- H_k{}^T + R_k)^{-1} \qquad (25)$$

$$P_k = (I - K_k H_K) P_k^- \tag{26}$$

The CKF will be optimal only if the noise matrices are accurately known, otherwise it will lose the optimal capability. Therefore, Sage-Husa AKF is used to improve the optimal performance of the filter by changing the noise matrices in real time inside the filter loop. The noise matrices are modified as [13]

$$q_{k+1} = (1-d_k) q_k + d_k \Xi_k (x_k^- - \Phi_{k-1} x_{k-1}^-)$$

$$Q_{k+1} = (1-d_k) Q_k + d_k \Xi_k [K_k \Lambda_k \Lambda_k^T K_k^T + P_k - \Phi_{k-1} P_{k-1} \Phi_{k-1}^T] \Xi_k^T$$

$$r_{k+1} = (1-d_k) r_k + d_k [z_k - H_k x_k^-]$$

$$R_{k+1} = (1-d_k) R_k + d_k [(z_k - H_k \Phi_k \hat{x}_k^-)(z_k - H_k \Phi_k \hat{x}_k^-)^T]$$

Where $\Xi_k = (\Gamma_k^T \Gamma_k)^{-1} \Gamma_k^T$, $d_k = (1-b)/(1-b^{k+1})$ and $\Lambda_k = z_k - H_k \Phi_k \hat{x}_k^- - r_k$. The value of *b* is obtained by experiment and takes the value as $0 < b < 1$.

4.1. INS/GPS Integration

INS attitude, velocity, position and sensor errors are selected as the states of the system. The system error model can be expressed in the form of a linear stochastic equation as

$$\dot{x}(t) = Fx(t) + W(t) \tag{27}$$

The model of the INS/GPS integrated system is obtained by combining Eq-11 and Eq-27 and discretizing to get

$$x_k = \Phi_{k-1} x_{k-1} + W_k \tag{28}$$

Where x_k is the states vector and Φ_k is the discrete state transition matrix obtained from Equations 1- 4 and 10. W_k is the uncorrelated white noise of the INS sensors and GPS clock.

$$x = \begin{bmatrix} \phi^T & (\delta v^n) & \delta p^T & \varepsilon^b & \nabla^b & \delta b_r & \delta d_r \end{bmatrix}^T \tag{29}$$

The measurement model of the integrated system is given in Eq-18. The initial state vector, error covariance matrix and the process noise matrices are selected as

$$x_0 = [0_{1\times 17}]^T$$

$$P_0 = diag(\begin{bmatrix} \phi_0 & \delta v_0^n & \delta p_0 & \varepsilon_0^b & \nabla_0^b & \beta_\rho & \beta_{\dot{\rho}} \end{bmatrix}^2)$$

$$Q_0 = diag(\begin{bmatrix} \sigma_{w\varepsilon}^2 & \sigma_{w\nabla}^2 & 0_{1\times 6} & 0_{1\times 5} \end{bmatrix})$$

Where β_ρ, $\beta_{\dot{\rho}}$ are GPS clock bias and drift errors. $\sigma_{w\varepsilon}^2$, $\sigma_{w\nabla}^2$ are the variances of gyro and accelerometer random noises.

5. Real Data Results

A field test was performed to collect the real data of a low accuracy *STIM300* MEMS based IMU and a single frequency *NovAtel* GPS receiver installed on a land navigation

vehicle with a known lever arm. IMU raw data is sampled at 100 Hz while GPS data is collected at 1Hz. The measurement data of the two systems is fused through the Adaptive KF using the tightly coupled approach in a closed loop. The value of *b* is chosen as 0.98 in this integration process to scale the noise matrices for optimal estimation. Non-holonomic constraints are not used in this scheme. The generated moving trajectory track of the vehicle is shown in Fig-3. Integration results of the system are illustrated in Fig-4 to Fig-8 which reflects a remarkable improvement in the attitude, velocity and position parameters of the INS/GPS. However, initially large azimuth error is seen in Fig-4 due to the bad observability in initial static mode of the system. The azimuth error starts converging when the vehicle starts moving as depicted in Fig-5 and limits it to less than ± 20 arc-minutes in the whole navigation run. The velocity error is significantly reduced to the best accuracy level. Position error, compensated for lever arm effect is accurately reduced to ± 4 m in latitude, longitude and height. Fig-8 shows the difference between the gyro constant drift and the drift estimated by the filter. The filter keeps it close to the zero level in the low cost MEMS-INS during the whole navigation period.

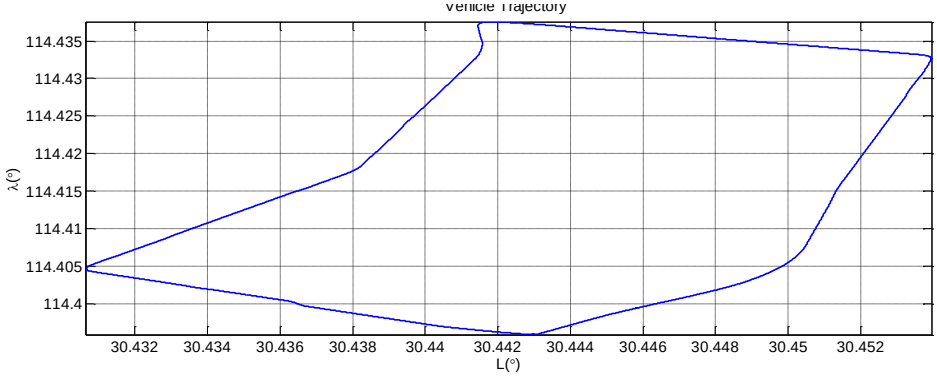

Figure 3. Trajectory

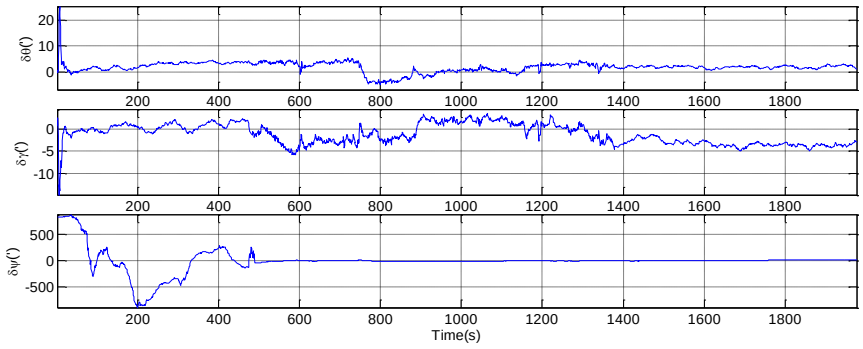

Figure 4. Attitude Error

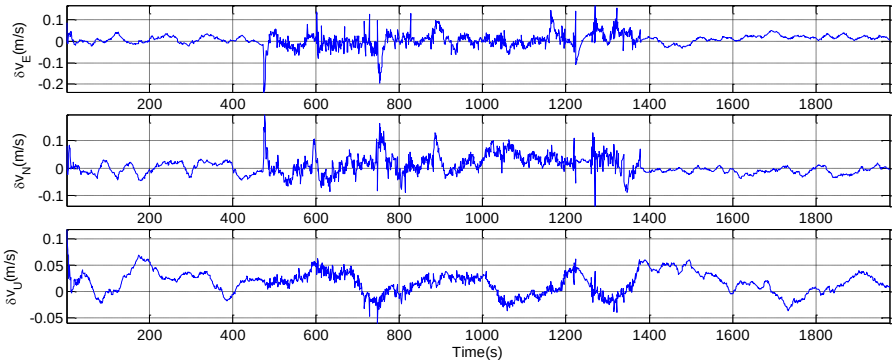

Figure 5. Azimuth Error

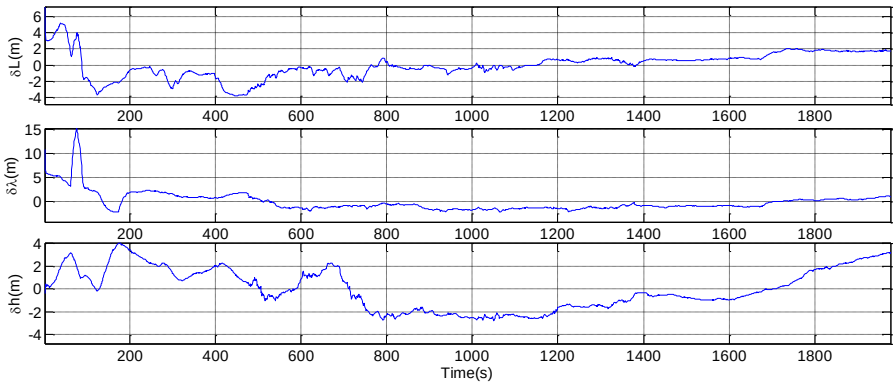

Figure 6. Velocity Error

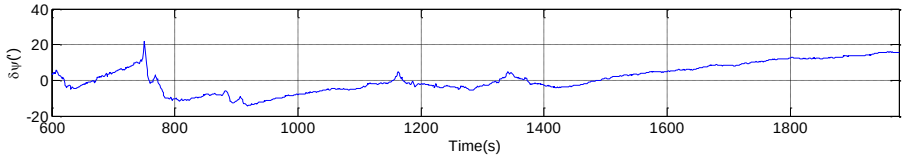

Figure 7. Position Error

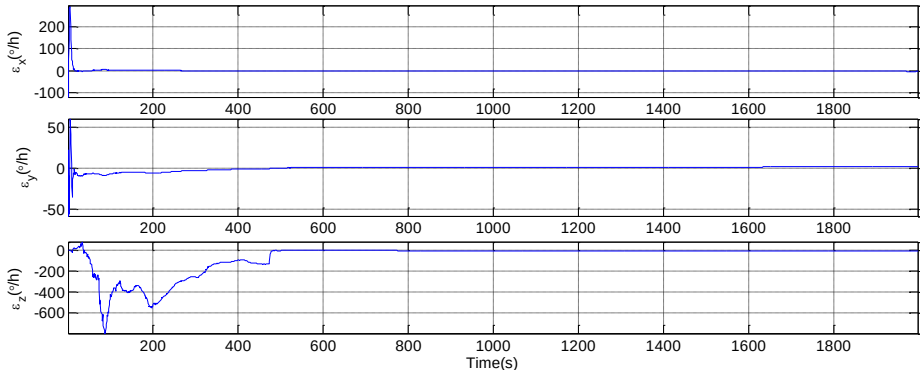

Figure 8. Gyro Drift

6. Conclusion

This paper has discussed a tightly coupled scheme and its implantation for the integration of a low-cost MEMS-INS and a GPS. In this model, a continuous measurement data is produced to the filter even if only one satellite signal is tracked. However, it has one main drawback that it can produce no inherent stand-alone GPS solution. Sage-Husa AKF is used to improve the performance of the CKF by scaling the system noises in real time and increased the stability of the filter. The AKF optimally merged the data of the two systems and showed better performance than CKF. The integration results well demonstrated the performance and effectiveness of the developed scheme.

References

[1] A. Angrisano, "GNSS/INS Integration Methods", Calgary Alberta, **(2010)**.
[2] N. El-Sheimy and X. Niu, "The Promise of MEMS to the Navigation Community", (**2007)**, pp. 26-56.
[3] E. Shin, "Estimation Techniques for Low-Cost Inertial Navigation", Department of Geomatics Engineering, University of Calgary, Canada, UCGE Report No. 20219, **(2005)**.
[4] E. Poh, A. Koh and X. Yu, "Integration of Dead Reckoning Sensors with MEMS IMU", Proceeding of ION GPS, **(2002)**, pp. 1148-1152.
[5] P. Misra and P. Enge, "Global Positioning System Signals, measurements and performance", Ganga-Jamina Press.Misra and Enge, **(2001)**.
[6] R.M. Rogers, "Applied Mathematics in Integrated Navigation Systems, American Institute of Aeronautics and Astronautics, Inc., **(2000)**.
[7] M. Brenner, "Integrated GPS/Inertial Fault Detection Availability", Proceedings of ION GPS, **(1995)**, Palm Springs CA, US, pp. 1949-1958.
[8] Y. Yang, "Tightly Coupled MEMS INS/GPS Integration with INS Aided Receiver Tracking Loops", Ph.D. Thesis, Calgary, Alberta, May **(2008)**.
[9] D.T. Knight, "Rapid Development of Tightly Coupled GPS/INS Systems", In Aerospace and Electronic Systems Magazine, vol. 12, no. 2, IEEE, **(1999)**, pp. 14-18.
[10] M.G. Petovello, "Real-Time Integration of a Tactical-Grade IMU and GPS for High-Accuracy Positioning and Navigation", Department of Geomatics Engineering, University of Calgary, Canada, UCGE Report No. 20173, **(2003)**.
[11] C. Hide, T. Moore and M. Smith, "Adaptive Kalman Filtering Algorithms for Integrating GPS and Low Cost INS", Proceeding in IEEE, **(2004)**.
[12] C. Hu, W. Chen,Y. Chen and D. Liu, "Adaptive Kalman Filtering for Vehicle Navigation", Journal of Global Positioning Systems , **(2003),** vol. 2, no. 1, pp. 42-47.
[13] W. Gao, J. Li, "Adaptive Kalman filtering for the Integrated of SINS/DVL System", Journal of Computational Information System, vol. 9, no. 16, **(2013)**, pp. 6443-6450.
[14] D.H. Titteron and J. Weston, "Strapdown Inertial Navigation Technology, 2nd Ed, Institute of Electrical Engineers", UK, **(2005)**.
[15] R. Kenneth, "Britting, Inertial Navigation Systems Analysis", Wiley-Interscience, New York, **(1971)**.
[16] P. Yang, Y. Qin and G. Yan, "Local Feedback Compensation Method for INS/GPS/OD Land Navigation System", Proceedings of the IEEE **(2008)**, International Conference on Information and Automation.
[17] M. Kayton and W.R. Fried, "Avionics Navigation Systems", John Wiley and Sons, New York, **(1997)**.
[18] D. Ellio, and Kaplan, :GPS Theory and Application, Beijing, Publishing House of Electronic Industry", **(2002)**.

